Environmental Science & Technology

Article

pubs.acs.org/est

Biogeochemical Controls on the Product of Microbial U(VI) Reduction

Malgorzata Stylo,[†] Daniel S. Alessi,[†] Paul PaoYun Shao,[†] Juan S. Lezama-Pacheco,[‡] John R. Bargar,[§] and Rizlan Bernier-Latmani[†,*]

[†]Environmental Microbiology Laboratory, École Polytechnique Fédérale de Lausanne, CH-1015, Lausanne, Switzerland

[‡]School of Earth Sciences, Environmental Earth System Science Department, Stanford University, Stanford, California 94305-4216, United States

[§]Chemistry and Catalysis Division, Stanford Synchrotron Radiation Lightsource, SLAC National Accelerator Laboratory, Menlo Park, California 94025, United States

Supporting Information

ABSTRACT: Biologically mediated immobilization of radionuclides in the subsurface is a promising strategy for the remediation of uranium-contaminated sites. During this process, soluble U(VI) is reduced by indigenous microorganisms to sparingly soluble U(IV). The crystalline U(IV) phase uraninite, or UO_2, is the preferable end-product of bioremediation due to its relatively high stability and low solubility in comparison to biomass-associated nonuraninite U(IV) species that have been reported in laboratory and under field conditions. The goal of this study was to delineate the geochemical conditions that promote the formation of nonuraninite U(IV) versus uraninite and to decipher the mechanisms of its preferential formation. U(IV) products were prepared under varying geochemical conditions and characterized with X-ray absorption spectroscopy (XAS), scanning transmission X-ray microscopy (STXM), and various wet chemical methods. We report an increasing fraction of nonuraninite U(IV) species with decreasing initial U concentration. Additionally, the presence of several common groundwater solutes (sulfate, silicate, and phosphate) promote the formation of nonuraninite U(IV). Our experiments revealed that the presence of those solutes promotes the formation of bacterial extracellular polymeric substances (EPS) and increases bacterial viability, suggesting that the formation of nonuraninite U(IV) is due to a biological response to solute presence during U(VI) reduction. The results obtained from this laboratory-scale research provide insight into biogeochemical controls on the product(s) of uranium reduction during bioremediation of the subsurface.

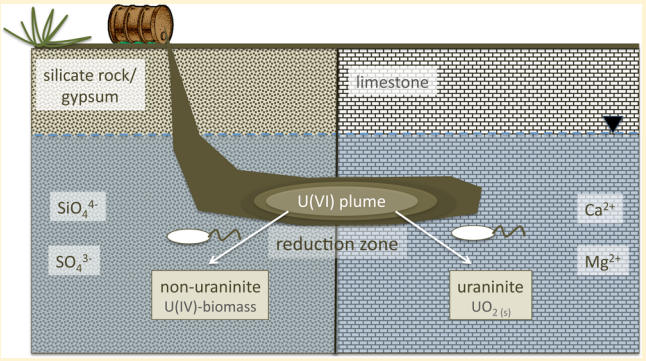

1. INTRODUCTION

Decades of uranium mining and processing, as well as nuclear power generation and weapons production, resulted in U contamination at many sites across the world. This contamination raises environmental and public health concerns primarily due to the chemical toxicity of uranium. Since U is not degradable, strategies for its remediation at field sites rely on decreasing its mobility and bioavailability in situ. A particularly successful approach is the stimulation of indigenous soil or aquifer bacteria by the injection of an electron donor into the U-contaminated subsurface.[1−3] This promotes the microbially driven reduction of the relatively soluble U(VI) species to less soluble U(IV),[4−7] thus decreasing the mobility and bioavailability of U in the aquifer.[8] It has recently been found that under field relevant conditions, uraninite (UO_2) is not the sole bioreduced U species, as was previously believed. Noncrystalline, biomass-associated nonuraninite U(IV) species were found to be a common product of microbial U(VI) reduction.[9−11]

It is essential to understand that, in the literature, what is referred to as "bio-UO_2" (microbially produced uraninite), is actually a mixture of both species: crystalline uraninite and amorphous nonuraninite U(IV).[12] Depending on the geochemical conditions present during U(VI) reduction, the ratio of the two U(IV) species can vary. Laboratory-scale research showed that it is possible to control this ratio.[9] In a simple medium (containing only bicarbonate and PIPES buffer) approximately a 50/50 mixture of the two species is the product of U(VI) reduction mediated by the metal-reducing microorganism *Shewanella oneidensis* MR-1. Conversely, non-

Received: June 14, 2013
Revised: October 3, 2013
Accepted: October 9, 2013
Published: October 9, 2013

Table 1. Sample List Describing the Medium Composition and Concentration of Added Uranium for Each Reduction Batch

		BP (simple medium 30 mM bicarbonate, 20 mM PIPES) additions:						
sample name	U concentration (μM)	SO_4^{2-}(mM)	SiO_4^{4-}(mM)	Mg^{2+} (mM)	Ca^{2+} (mM)	PO_4^{3-}(mM)	NaCl (mM)	Rifle ground water
BP 100	100	–	–	–	–	–	–	–
BP 200	200	–	–	–	–	–	–	–
BP 400	400	–	–	–	–	–	–	–
BP 600	600	–	–	–	–	–	–	–
S-1	400	1	–	–	–	–	–	–
S-2	400	10[a]	–	–	–	–	–	–
Si-1	400	–	0.3[a]	–	–	–	–	–
Si-2	400	–	1	–	–	–	–	–
Mg	400	–	–	5[a]	–	–	–	–
Ca-1	400	–	–	–	0.7	–	–	–
Ca-2	400	–	–	–	7[a]	–	–	–
P-1	100	–	–	–	–	0.02	–	–
P-2	100	–	–	–	–	0.2	–	–
Ca/P	100	–	–	–	0.7	0.2	–	–
Ca/P-2	100	–			2.1	2.1	–	–
Na	400	–	–	–	–	–	86	–
RGW	400	–	–	–	–	–	–	+

[a]Environmentally relevant concentration, based on Rifle Ground Water (Colorado, U.S., Campbell et al, 2011).

uraninite U(IV) is formed predominantly by the same microorganism in a more complex, higher ionic strength (IS), salt rich medium. Nonuraninite species, as the name suggests, are the U(IV) species that lack the crystalline form of the mineral uraninite. That includes amorphous U(IV) phases, characterized by a structural decrease or complete absence of the U−U pair at 3.8 Å, as observed in Extended X-ray Absorption Fine Structure Spectra (EXAFS).[9,13] Moreover, previous studies suggested that nonuraninite U(IV) species also represent U(IV) complexes bound to biomass, through P-containing ligands.[9]

For the purposes of bioremediation, the preferable end-product of U(VI) bioreduction is the sparingly soluble mineral uraninite due to its greater resistance to oxidation and complexation,[12,14] as compared to labile nonuraninite U(IV) species. In order to design engineering techniques (solutions) that lead to the preferential formation of uraninite in the subsurface, it is essential to understand the fundamental controls over this process. For that reason, in this work, we investigate the specific geochemical and biological conditions that drive the preferential formation of nonuraninite U(IV). In particular, we probe whether: (a) a higher ionic strength could promote the formation of nonuraninite U(IV) species; (b) the presence of specific solutes, that influence the electrostatics of the bacterial cell wall, promotes the association of U(IV) species to the biomass and prevents the precipitation of crystalline UO_2; and (c) the solutes present could affect bacterial viability and production of extracellular polymeric substances (EPS), which can act as sorption and nucleation sites, and mediate U(VI) reduction.[15]

We report three primary results: (1) the presence of dissolved solutes in the reduction media or groundwater, particularly phosphate, silicate, and sulfate, have a significant effect on the resulting U(IV) species. (2) These solutes do not associate with the U(IV) species formed or biomass; rather, they impact the cells, and the resulting biological response promotes the formation of one or the other U(IV) product. (3) Additionally, the initial concentration of U(VI) impacts the U(IV) product: a decreasing concentration of uranium correlates with an increase in the fraction of nonuraninite U(IV) species formed.

2. MATERIALS AND METHODS

2.1. Microbial Uranium Reduction Conditions. Biomass associated uranium U(IV) was produced as previously described in Bernier-Latmani et al.[9] *Shewanella oneidensis* MR-1 cultures were grown in sterile Luria−Bertani broth (LB medium) until they reached midexponential phase. Cells were harvested by centrifugation at 8000*g* for 10 min and washed in simple buffered medium (referred to as BP medium), composed of 30 mM $NaHCO_3$ and 20 mM 1,4-piperazinediethanesulfonic acid (PIPES buffer) adjusted to pH 6.8. Washed cells were suspended to an optical density (OD_{600}) of 1.0 in BP medium amended with solutes as described in Table 1, or in filter-sterilized groundwater from a U-contaminated site at Old Rifle, Colorado[16] (RGW) (Table 1).

2.2. Experimental Design. Our experimental design was based on the observation that *S. oneidensis* MR-1 can reduce U(VI) to bio-UO_2 or, in the presence of solutes, to nonuraninite U(IV) species.[9] As was discussed above, it is crucial to remember that bio-UO_2 is a mixture of crystalline uraninite and amorphous nonuraninite U(IV) species.[12] However, depending on the chemical composition of the reduction medium, the ratio of the two U(IV) species can vary. Therefore, to identify conditions that lead predominantly to the formation of nonuraninite U(IV) species, we conducted U(VI) bioreduction experiments in BP medium amended with individual solutes or mixtures thereof. Duplicate reduction batches with the appropriate solute composition were amended with 20 mM lactate as an electron donor and varying concentrations of U(VI) acetate (100 to 600 μM) as a source of U(VI) under anoxic conditions. The relatively high concentrations of uranium (in comparison to field concentration ranging from 0.4 to 1.8 μM [16]) was necessary in order to allow sufficient U(IV) accumulation for Scanning Transmission X-ray Microscopy (STXM) characterization. Our model systems were amended with 30 mM bicarbonate, and a circumneutral pH was set in order to maintain the added dissolved U(VI) in the aqueous phase. According to the

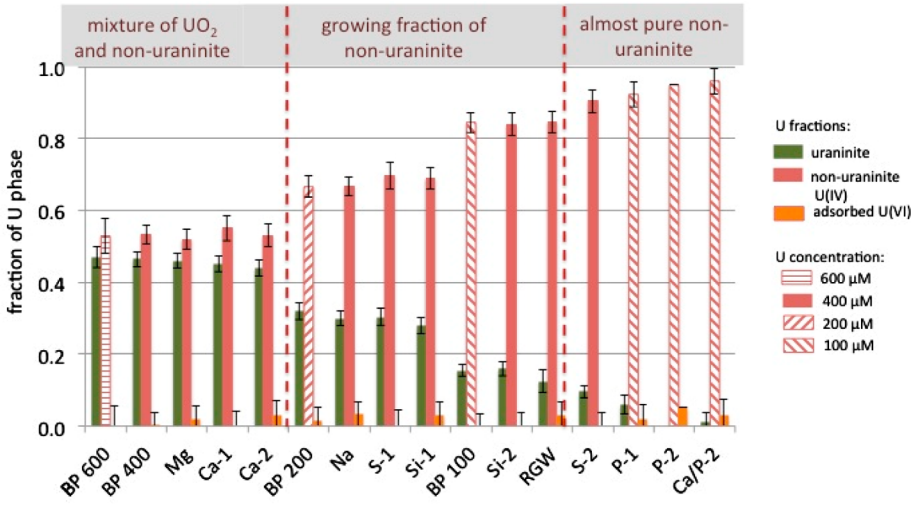

Figure 1. Linear combination fits (LCF) of EXAFS spectra for the studied conditions. The samples are organized by increasing fraction of nonuraninite species in the sample. Error bars represent the variation for each fraction calculated by the fitting program (Athena[20]).

chemical speciation calculations (Figure S3 in the Supporting Information, SI), that resulted in a predominance of the uranium(VI) carbonate complexes—$UO_2(CO_3)_2^{2-}$, one of the main U(VI) aqueous species found in the groundwater as well.[16] In addition, batch duplicate conditions containing RGW also were prepared. The initial U(VI) concentration was lowered to 100 μM in all batches containing phosphate, in order to avoid U(VI) precipitation.[17] The details of all the experimental batches are listed in Table 1.

2.3. Quantification of Uranium, Calcium, and Phosphate. Subsamples were taken over time from each batch to quantify dissolved uranium, calcium and phosphate. Samples were filtered though 0.22 μm membranes and the filtrates were refrigerated until analysis. The concentrations of uranium and calcium in subsamples were diluted in 0.1 M nitric acid and measured by inductively coupled plasma optical emission spectrometry (ICP-OES). Phosphate was quantified spectrophotometrically with a modified ascorbic acid method.[18] Briefly, 0.3 mL of sample were mixed with 0.7 mL of reagent (1 mL of 100 mg/L ascorbic acid and 6 mL of 4.2 g/L ammonium molybdate in sulfuric acid) and incubated at 55 °C for 10 min. The concentration of P was determined by measuring the absorbance at 820 nm with a UV-2501 PC Shimadzu spectrophotometer.

2.3. X-ray Absorption Spectroscopy (XAS). Uranium X-ray absorption spectroscopy (XAS) measurements of samples were conducted at beamline 4−1 of the Stanford Synchrotron Radiation Lightsource (SSRL) at the Stanford Accelerator Laboratory (SLAC). Each sample was filtered through a 0.22 μm filter prior to analysis and the retained, concentrated solid phase was mounted in aluminum holders with Kapton windows and kept under anoxic conditions prior to and during analysis. The samples were maintained in a liquid N_2 cryostat during analysis, and kept under a vacuum of approximately 10^{-6} Torr. X-ray absorption spectra were collected at the U L_{III}-edge (17 166 eV), in fluorescence and transmission modes. A double-crystal Si (220) monochromator was used to select the energy over each sweep, and was slightly detuned to reject higher energy harmonics. An yttrium metal foil was used for the initial and internal calibration, with its first derivative set to 17 038.4 eV. EXAFS spectra were processed using the SixPACK[19] and Athena[20] analysis packages. Backscattering phase and amplitude functions used to fit the spectra were generated in Artemis using FEFF6L.[21] The EXAFS spectra were also fit by linear combination fitting[20] (LCF) using previously characterized compounds as reference samples: biogenic uraninite (free from nonuraninite U(IV) species as a result of bicarbonate wash, details in the SI), nonuraninite U(IV) and adsorbed U(VI) (details in the SI, Figure S2 and Table S1).

2.4. Scanning Transmission X-ray Microscopy (STXM). *2.4.1. Sample Preparation.* Anaerobic samples were placed in serum bottles sealed with butyl rubber stoppers and crimped with an aluminum seal. The serum bottles were shipped in a hermetically sealed stainless steel shipping canister (Schuett-biotec GmbH, Göttingen, Germany) filled with N_2 to a slightly positive pressure. Samples (1.0 μL) were loaded on silicon nitride microporous TEM window grids (TEMwindows, West Henrietta, NY, U.S.) and allowed to settle for 5 min before excess liquid was wicked away. Grids were mounted on holders with four very small dollops of epoxy.

2.4.2. Data Collection. Carbon speciation and uranium localization analyses by scanning transmission X-ray microscopy were conducted on the STXM end station 11.0.2.2 of the Molecular Environmental Science beamline 11.0.2 at the Advanced Light Source (ALS)[22] with the synchrotron storage ring operating at 1.9 GeV and 500 mA multibunch mode storage current. A 150 l mm^{-1} grating and 20 μm exit slit used for carbon K-edge imaging and spectroscopy. A 1200 l mm^{-1} grating and 30 μm exit slit were used for uranium $4d_{5/2}$ edge imaging and spectroscopy.[23] Carbon K-edge energy calibration was accomplished using the 3p Rydberg peak at 294.96 eV of gaseous CO_2.[24] Carbon speciation stacks were collected through serial image collection along C K-edge energies (280−300 eV). Uranium localization maps were collected at 725 and 738 eV below and at the edge, respectively. Carbon reference spectra of albumin (protein), dipalmitoyl-*sn*-glycero-3-phosphocholine (DPPC) (lipid) and alginic acid (polysaccharide) were recorded along the C K-edge (280−300 eV). The uranium reference spectrum was collected along its $4d_{5/2}$ edges (720 − 780 eV), capturing both peaks in that range. All of the spectra were normalized to an optical density (OD) corresponding to a 1-nm layer.

2.4.3. Data Processing. Using the aXis2000 software package[25] both carbon stacks and uranium maps were

converted from transmission data to OD. They were then iteratively aligned to convergence by cross-correlation using the Jacobsen stack analyze algorithm[26] with the highest energy image as a reference. Quantitative C-speciation maps were calculated from the aligned image stacks by singular value decomposition using the stack-fit routine in aXis2000. Each pixel was fit with a linear combination of the three normalized reference spectra (albumin (protein), DPPC (lipid), alginic acid (polysaccharide)) plus a constant. Composite maps were obtained by overlaying the protein (red), lipid (green), and polysaccharide (blue) maps using an RGB additive color intensity scale. Uranium localization maps were obtained by subtracting the aligned below edge (725 eV) image from the above edge (738 eV) image.

2.5. Zeta Potential Measurement. Samples (1 mL) were taken from selected reduction batches and inserted into disposable capillary cuvettes (Malvern). Measurement of zeta potential was made on the ZetaSizer Nano (Malvern). Zeta potential (ζ) measurements represent the electrical potential extant at the shear plane, which corresponds to a small distance away from the surface. For bacteria, the zeta potential is linked to the surface charge of the bacterium and, indirectly, to the biomolecules present at the surface of the bacterium.

3. RESULTS AND DISCUSSION

Figure 1 and Table S7 (in the SI) summarize the results of the linear combination fits (LCF)[20] of EXAFS spectra for U(IV) products formed under the sixteen conditions considered (listed in Table 1). Ca/P was used as a nonuraninite U(IV) reference for the LCF, as the product of U(VI) reduction under that condition was pure nonuraninite U(IV) (details in the SI, Table S1). Our results confirm that the biouraninite is indeed a mixture of uraninite and nonuraninite U(IV) species, in an approximately 1:1 ratio, formed under simple conditions similar to those examined in past studies[9,12] (sample BP 400). The geochemical conditions can be divided into three groups based on the contribution of the nonuraninite U(IV) fraction in comparison to the baseline case, BP 400 (previously studied[9,12]). An even higher U concentration (BP 600) or the addition of calcium or magnesium (Ca-1, Ca-2, and Mg) do not alter the U(IV) product. The second group of geochemical conditions that includes lower U concentrations (BP 200 and BP 100) or the presence of certain solutes (Na, S-1, Si-1, Si-2) displays an increase in the nonuraninite U(IV) fraction. The third group corresponds to an almost pure nonuraninite U(IV) product and the geochemical conditions represent the presence of phosphate (P-1, P-2, Ca/P-2) as well as a high sulfate concentration (S-2). The results obtained with XAS were confirmed using an extraction method (with 1 M bicarbonate, described in the SI) to characterize the U(IV) end products (Figure S1 in the SI). Results show that both methods support similar findings: the highest nonuraninite U(IV) fraction is formed in the presence of phosphate, silicate and sulfate (details in the SI).

3.1. U Concentration-Dependent U(IV) Product Formation. Our results revealed that with increasing total U concentrations, up to 400 μM, the fraction of crystalline uraninite in the reduced product increases. A further increase in U concentration does not alter the composition of the U(IV) product (BP 600). The U concentration-dependent U(IV) product formation could be a result of the saturation of the binding sites on the bacterial surface. On the basis of the suggested model for nonuraninite U(IV) formation that implies binding of monomeric U(IV) with phosphate,[9] we expect U(IV) to be associated with bacterial phosphate groups. The outer membrane of Gram-negative bacteria (including the studied *Shewanella oneidensis*) consists of lipopolysaccharides and phospholipids that are able to bind nanocrystalline U(IV) species.[27] Hence, we propose that when a high concentration of U is present, a fraction of reduced uranium ions that correspond to nonuraninite U(IV) associate with phosphate functional groups on the biomass, saturating the available sites, and the remaining fraction precipitates to form crystalline uraninite. Hence, the greater the initial U concentration becomes, the greater the uraninite fraction present in the system. Conversely, when a low U-concentration is present, most of the U(IV) ions can sorb onto the biomass, yielding a relatively higher fraction of nonuraninite U(IV) species in the end product.

3.2. Influence of Ionic Strength. The EXAFS results provided an answer to the first question we posed: whether the relatively higher ionic strength of the medium that produces predominantly nonuraninite U(IV)[12] was responsible for its preferential formation. The LCF show that a higher IS (obtained by addition of 86 mM NaCl to BP, condition Na) resulted in an increase of the nonuraninite U(IV) fraction in the end product, from 55% to 68% (Figure 1) but did not account for the full extent of the preferential formation of nonuraninite U(IV) species (corresponding to 90% nonuraninite U(IV) as reported in Alessi et al.[12]). Hence, IS may play a role in favoring nonuraninite U(IV) formation but its effect is not sufficient to account for the entirety of the nonuraninite U(IV) formed. Moreover, the impact of NaCl under realistic environmental conditions (NaCl on the order of 10 mM in comparison to tested 86 mM) is likely insignificant.

3.3. Role of Specific Solutes. On the basis of the observation described above, we focused on the role of a subset of the original solutes during U(VI) bioreduction. The five solutes considered (sulfate, silicate, magnesium, calcium, and phosphate) were selected due to their environmental relevance to the Old Rifle site in Colorado, as well as their general importance in environmental systems. Calcium, silicate, magnesium, and sulfate are present in Old Rifle at concentrations of 7 mM, 0.3 mM, 5 mM, and 10 mM, respectively.[16] Additionally, calcium is well-known for its property to inhibit or decrease the rate of microbial U(VI) reduction.[28−30] Phosphate, however, has been shown to be important in nonuraninite U(IV) formation.[31] A recent report showed that the formation of nonuraninite U(IV) [also referred to as mononuclear U(IV)] was dependent on the presence of phosphate—for several strains (*Desulfitobacterium* spp. and *S. putrefaciens*).[13] Moreover, coordination of U(IV) to phosphate has been invoked to fit EXAFS data corresponding to nonuraninite U(IV).[9,12,31]

The five solutes had different impacts on the fraction of nonuraninite U(IV) formed. The environmentally relevant concentration of cations—calcium and magnesium—were shown to have no effect on the composition of the U(IV) product. However, the presence of anions (in addition to the background concentration of bicarbonate that was constant for all of the studied cases) was revealed to have a significant influence on the U(IV) product composition. The environmentally relevant concentration of sulfate (10 mM) increased the contribution of nonuraninite U(IV) from 55% to 90%. In the case of silicate, the presence of 0.3 mM results in a relatively small increase of nonuraninite U(IV) species (from 55% to

70%). However, a higher concentration (1 mM) impacted the fraction of nonuraninite U(IV) significantly (increasing it from 55% to 85%). Despite its low concentration in the Rifle groundwater, silicate is of interest due to its ability to alter U minerals[32] and diminish uraninite corrosion by slowing down the uranium loss rates,[16] and therefore, it should be taken into account when considering environmental conditions at the U-contaminated site.

In contrast to the other solutes, even low concentrations of phosphate (i.e., 0.02 and 0.2 mM) promote the predominant formation of nonuraninite U(IV) species (92–95%). Addition of calcium (0.7 mM or 2.1 mM) to phosphate (0.2 mM) results in a similar product—almost purely nonuraninite U(IV) species, confirming no significant influence of added calcium ions. However, the sample (Ca/P) was used as an end member representative of nonuraninite U(IV) species in LCF due to the absence of a U–U pair that was confirmed by EXAFS fitting (details in the SI, Table S1).

The results revealed the influence of orthophosphate (as well when combined with Ca^{2+}) on U(IV) product formation; however, the mechanism of this influence remained elusive. Our initial hypothesis was that Ca^{2+} and/or HPO_4^{2-} could associate with bacterial cell walls, thus altering their surface properties and precluding uraninite formation. Alternatively, association of phosphate with U(IV) may preclude the precipitation of UO_2 and promote the formation of noncrystalline U(IV) species, in a manner akin to the delayed transformation of less structured ferrihydrite into crystalline phases due to the presence of phosphate.[33,34] These hypotheses are predicated on the notion that the two solutes are complexed with the cell biomass. However, measurements of the solution concentration of Ca^{2+} and HPO_4^{2-} during U(VI) bioreduction revealed that the concentrations remained constant over time (Figure 2). Moreover, complexation of U(VI) by Ca^{2+} and

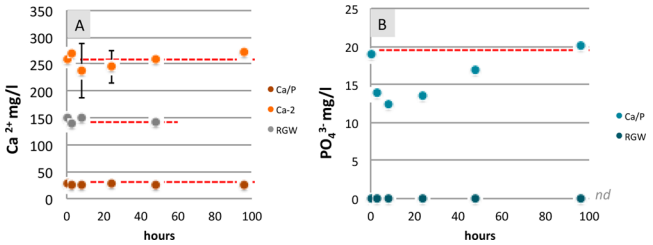

Figure 2. Concentration of the dissolved ions: (A) calcium and (B) phosphate during the bioreduction of U(VI) over time. The error bars represent the variability based on duplicates. Red dashed lines depict initial concentrations of solutes. The decrease in phosphate concentration overtime followed by an increase is attributed to the uptake of phosphate by cells during metabolic activity followed by its release upon cell lysis. The overall conclusion is that phosphate is not associated with U since U remains associated with cells and cell fragments after lysis. *nd*, not detectable values of phosphate for the RGW.

HPO_4^{2} is limited due to the predominant formation of the U(VI)-carbonate complexes (SI Figure S3). This suggested that there is limited association of these ions with biomass, U(VI) or formed U(IV) species, resulting in minimal impact of phosphate and calcium on cell wall electrostatics. The fluctuation of dissolved phosphate ions during the U(VI) reduction may be attributed to bacterial uptake during active metabolism and release following cell lysis.

To investigate in more detail the surface behavior of the biomass-U system in the presence of these solutes, zeta potential (ζ) measurements were performed for select samples. Unlike many Gram-negative bacteria, including most *Shewanella* strains with ζ values ranging from −30 to −40 mV, *S. oneidensis* MR-1 cells possess a relatively low surface charge: a few mV at circumneutral pH and an ionic strength of 0.01.[35] Our results confirm previous findings (Table 2), with surface

Table 2. Zeta Potential Values for Bacterial Biomass During U(VI) Bioreduction under Varying Geochemical Conditions over Time

	Zeta potential [mV] over time		
	1 h	1 day	4 days
Ca/P	−3.97	−17.2	−29.3
BP 100	−3.2	−3.69	−6.95
BP 400	−3.25	−4.5	−6.19
Ca-2	−3.43	−2.6	−4.16
Na	−3.57	−4.98	−5.3
Si-1	−3.21	−5.79	−6.65

charge values ranging from −3.2 to −3.9 mV for *S. oneidensis* MR-1 in the initial stage of the experiment. Interestingly, the zeta potential becomes more negative during the course of microbial U(VI) reduction. The greatest change in zeta potential over time was observed when both Ca^{2+} and HPO_4^{2-} were present, and was correlated with the production of the highest fraction of nonuraninite U(IV) species of all conditions.

The reason for the initial lower surface charge of strain MR-1 is attributed to the structure of its lipopolysaccharides (LPS) that exhibit an unusual component, 8-amino-3-deoxy-D-manno-octulosonic acid (8-amino-Kdo).[36] In this type of LPS, amino groups shield the charge of the carboxylate groups, which are usually responsible for higher surface charge in other Gram-negative bacteria. However, bacterial exopolymeric substances (EPS) also exhibit a negative charge.[37,38] Therefore, EPS formation could lead to more negative zeta potential values for the biomass as a whole. Indeed, one study revealed that the production of EPS by wild type *S. oneidensis* MR-1 yields a more negative surface charge (more negative electrophoretic mobility) compared to an EPS-deficient mutant.[39]

The findings presented in Table 2, showing more negative bacterial surface charges during U(VI) reduction (only in the presence of phosphate, with addition of calcium), suggest a possible biological response to the geochemical conditions leading to more negative surface charges. In particular, we were interested to find out whether this excursion in ZP could be attributed to the formation of bacterial EPS, as these polymers are proposed to host cytochromes involved in uranium reduction.[15]

3.4. Biological Controls. On the basis of the above findings, we formulated the hypothesis that the influence of solutes on the products of U(IV) reduction was indirect. We probed for evidence for EPS production using STXM, a method allowing the detection of carbon species (including the main components of EPS—lipids, proteins, and polysaccharides) along with the localization of uranium. We found little EPS production (Figure 3) in the case of the BP medium (for which a mixture of uraninite and nonuraninite are produced). However, in the case of BP amended with phosphate and addition of calcium (which leads to formation of nonuraninite

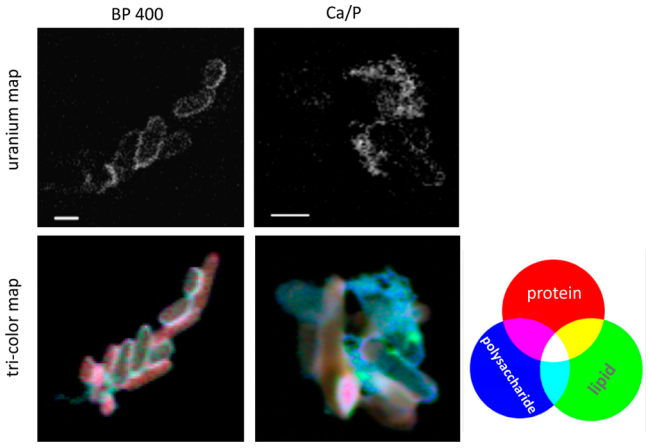

Figure 3. STXM images showing Uranium map and Tricolor map (indicating three main components of EPS: protein in red, lipid in green, and polysaccharide in blue) for U(IV) product formed in simple medium (BP 400) and with addition of phosphate and calcium (Ca/P).

U(IV)), extensive EPS production, rich in polysaccharides and lipids, is observed (Figure 3, SI Figure S4). The bulk extraction and quantification of EPS (SI Figure S5) support this finding: more carbohydrates are being produced when the two solutes (i.e., calcium and phosphate) are present. Most strikingly, the distribution of U in the two systems is distinct. In the EPS-poor case (BP-400), U is associated with the cell walls of bare cells (Figure 3). In contrast, in the EPS-rich case (Ca/P), U is associated primarily with the EPS itself (Figure 3). Additionally, results from viability tests (SI Figure S6) show that bacteria are able to survive better when phosphate and calcium are present in the medium. This suggests that cultures amended with the two solutes are in a more favorable physiological state than those without amendment.

We conclude that specific solutes such as sulfate (at 10 mM), silicate (at 1 mM) and phosphate (at 0.2 mM) have a similar impact on cell biomass as the complete medium (Widdel Low phosphate medium, as described in Alessi et al.[12]) that enhances nonuraninite U(IV). The geochemical composition of the reduction medium impacts EPS production, which in turn impacts U(IV) speciation and cell survival. It is, thus, not surprising that solutes typically associated with biological activity (sulfate and phosphate) impact nonuraninite U(IV) species formation more significantly than, for example, NaCl. Because silicate is considered a nonessential element for microbial nutrition, it is unclear why its presence would result in an improved physiological state that allows for EPS production. An additional major finding of this work is that the presence of orthophosphate is not necessary for the formation of nonuraninite U(IV), in contrast to previous reports (Boyanov et al.[13]). For example, an environmentally relevant concentration of sulfate (10 mM) is adequate to elicit the same contribution of nonuraninite U(IV) as phosphate (0.2 mM).

3.5. Environmental Relevance and Implications. We performed an additional experiment using groundwater from a U-contaminated site at Rifle (RGW). U(IV) formed under these field relevant conditions was found to be composed of approximately 80% nonuraninite U(IV) species and 20% UO_2 (Figure 1). Our result confirms previous findings that suggested the formation of nonuraninite U(IV) species associated with biomass during sediment-based bioremediation.[11] Comparing Rifle groundwater composition (that contains 5−6 mM of calcium, 8−9 mM of sulfate, 5 mM of magnesium, 8−9 mM of sodium, and 0.3 mM of silicate) with the solutes chosen for our systematic laboratory experiments, we were able to identify the potential and/or partial influence of sulfate (10 mM) and silicate (0.3 mM) promoting the formation of nonuraninite U(IV) under studied field conditions. Phosphate was not detected in RGW (Figure 2), consequently we were not able to assess its environmental impact. The results lend further support to the finding that the presence of orthophosphate in the medium is not a necessary condition for the formation of nonuraninite U(IV) species. Other common groundwater solutes appear to influence the U(IV) product to a similar extent. This result is consistent with field results showing the dominance of nonuraninite U(IV) as a product of U(VI) reduction despite the absence of measurable phosphate in the groundwater.[31]

Understanding the geochemical and biological aspects that govern the preferential production of nonuraninite U(IV) over crystalline uraninite is essential for planning bioremediation interventions at U-contaminated sites. The conclusions from our laboratory-scale research enabled us to pinpoint the role of specific solutes in the formation of nonuraninite U(IV) species under the selected geochemical conditions. Differences between our model system and the environment include typically lower concentrations of solutes and more complex geochemistry. However, capturing the complexity of the environmental sites exceeds the scope of this research. Nevertheless, our findings provide undisputable indication that certain (discussed above) geochemical conditions of the natural system influence U(IV) product formation. Therefore, this knowledge can be further applied to field investigations, allowing for a more accurate assessment of the environmental conditions, ongoing processes, and challenges related to the bioremediation of U-contaminated sites. For instance, bioremediation engineering techniques applied at a U-contaminated site in which the groundwater is dominated by calcium and magnesium solutes (such as in an aquifer overlying a limestone bedrock) may yield better results due to preferential uraninite formation. Conversely, in U-contaminated systems where the groundwater is rich in silicate and sulfate, such as might be expected in regions where the bedrock consists mainly of silicate minerals or gypsum (calcium sulfate), the predominant formation of nonuraninite U(IV) species may be expected. This environmental dependency however exposes a fundamental weakness of the bioremediation approach in natural systems and underscore the need for extended research on the further characterization of nonuraninite U(IV) species, in particular their formation mechanisms, resistance to the reoxidation and time dependent transformation to more crystalline uraninite.

■ ASSOCIATED CONTENT

Supporting Information

Additional wet chemical extraction data, EXAFS plots and fits to the spectra, viability graph, and bulk EPS quantification data. This material is available free of charge via the Internet at http://pubs.acs.org.

■ AUTHOR INFORMATION

Corresponding Author

*E-mail: rizlan.bernier-latmani@epfl.ch.

Notes

The authors declare no competing financial interest.

■ ACKNOWLEDGMENTS

We thank the Radiation Protection Group at the Stanford Synchrotron Radiation Lightsource for their support during the measurements, especially Marcia Torres, Carol Morris, and Darryl Murray. We thank Noemie Janot for help at the synchrotron. Also, we thank Prof. Tamar Kohn for the use of ZetaSizer. Work carried out at EPFL was funded by Swiss NSF Grant Nos. 200020_126821 and 200020_144335 and the SLAC Science Focus Area (FWP No. 10094) funded by the US DOE Subsurface Biogeochemical Research program. Portions of this research were carried out at the Stanford Synchrotron Radiation Lightsource, a national user facility operated by Stanford University on behalf of the U.S. Department of Energy (DOE), Office of Basic Energy Sciences and supported by the SSRL Environmental Remediation Science Program and BER-ERSD Project No. SCW0041. The SSRL Structural Molecular Biology Program is supported by the Department of Energy, Office of Biological and Environmental Research, and by the National Institutes of Health, National Center for Research Resources, Biomedical Technology Program. The Advanced Light Source is supported by the Director, Office of Science, Office of Basic Energy Sciences, of the U.S. Department of Energy under Contract No. DE-AC02-05CH11231. Beamline 11.0.2 is supported by the Director, Office of Science, Office of Basic Energy Sciences Division of Chemical Sciences, Geosciences, and Biosciences by the Condensed Phase and Interfacial Molecular Sciences Program of the U.S. Department of Energy at LBNL under Contract No. DE-AC02-05CH11231.

■ REFERENCES

(1) Anderson, R. T.; Vrionis, H. A.; Ortiz-Bernard, I.; Resch, C. T.; Long, P. E.; Dayvault, R.; Karp, K.; Marutzky, S.; Metzler, D. R.; Peacock, A. D.; White, D. C.; Lowe, M.; Lovley, D. R. Stimulating the in situ activity of *Geobacter* species to remove uranium from the groundwater of a uranium-contaminated aquifer. *Appl. Environ. Microb.* **2003**, *69*, 5884−5891.

(2) Banaszak, J. E.; Rittmann, B. E.; Reed, D. T. Subsurface interactions of actinide species and microorganisms: Implications for the bioremediation of actinide-organic mixtures. *J. Radioanal. Nucl. Chem.* **1999**, *241*, 385−435.

(3) Brookshaw, D. R.; Pattrick, R. A. D.; Lloyd, J. R.; Vaughan, D. J. Microbial effects on mineral-radionuclide interactions and radionuclide solid-phase capture processes. *Mineral. Mag.* **2012**, *76*, 777−806.

(4) Lovley, D. R.; Phillips, E. J. P.; Gorby, Y. A.; Landa, E. R. Microbial reduction of uranium. *Nature* **1991**, *350*, 413−416.

(5) Lovley, D. R.; Phillips, E. J. P. Reduction of uranium by *Desulfovibrio desulfuricans*. *Appl. Environ. Microbiol.* **1992**, *58*, 850−856.

(6) Lovley, D. R. Dissimilatory metal reduction. *Annu. Rev. Microbiol.* **1993**, *47*, 263−290.

(7) Burgos, W. D.; McDonough, J. T.; Senko, J. M.; Zhang, G. X.; Dohnalkova, A. C.; Kelly, S. D.; Gorby, Y.; Kemner, K. M. Characterization of uraninite nanoparticles produced by *Shewanella oneidensis* MR-1. *Geochim. Cosmochim. Acta* **2008**, *72*, 4901−4915.

(8) Borch, T.; Kretzschmar, R.; Kappler, A.; Van Cappellen, P.; Ginder-Vogel, M.; Voegelin, A.; Campbell, K. Biogeochemical redox processes and their impact on contaminant dynamics. *Environ. Sci. Technol.* **2010**, *44*, 15−23.

(9) Bernier-Latmani, R.; Veeramani, H.; Dalla Vecchia, E.; Junier, P.; Lezama-Pacheco, J. S.; Suvorova, E. I.; Sharp, J. O.; Wigginton, N. S.; Bargar, J. R. Non-uraninite products of microbial U(VI) reduction. *Environ. Sci. Technol.* **2010**, *44*, 9456−9462.

(10) Fletcher, K. E.; Boyanov, M. I.; Thomas, S. H.; Wu, Q. Z.; Kemner, K. M.; Löffler, F. E. U(VI) Reduction to mononuclear U(IV) by *Desulfitobacterium* species. *Environ. Sci. Technol.* **2010**, *44*, 4705−4709.

(11) Sharp, J. O.; Lezama-Pacheco, J. S.; Schofield, E. J.; Junier, P.; Ulrich, K.-U.; Chinni, S.; Veeramani, H.; Margot-Roquier, C.; Webb, S. M.; Tebo, B. M.; Giammar, D. E.; Bargar, J. R.; Bernier-Latmani, R. Uranium speciation and stability after reductive immobilization in aquifer sediments. *Geochim. Cosmochim. Acta* **2011**, *75*, 6497−6510.

(12) Alessi, D. S.; Uster, B.; Veeramani, H.; Suvorova, E.; Lezama-Pacheco, J. S.; Stubbs, J. E.; Bargar, J. R.; Bernier-Latmani, R. Quantitative separation of monomeric U(IV) from UO_2 in products of U(VI) reduction. *Environ. Sci. Technol.* **2012**, *46*, 6150−6157.

(13) Boyanov, M. I.; Fletcher, K. E.; Kwon, M. J.; Rui, X.; O'Loughlin, E. J.; Löffler, F. E.; Kemner, K. M. Solution and microbial controls on the formation of reduced U(IV) species. *Environ. Sci. Technol.* **2011**, *45*, 8336−8344.

(14) Cerrato, J. M.; Ashner, M. N.; Alessi, D. S.; Lezama-Pacheco, J. S.; Bernier-Latmani, R.; Bargar, J. R.; Giammar, D. E. Relative reactivity of biogenic and chemogenic uraninite and biogenic noncrystalline U(IV). *Environ. Sci. Technol.* **2013**, *49*, 9756−9763.

(15) Marshall, M. J.; Beliaev, A. S.; Dohnalkova, A. C.; Kennedy, D. W.; Shi, L.; Wang, Z.; Boyanov, M. I.; Lai, B.; Kemner, K. M.; McLean, J. S.; Reed, S. B.; Culley, D. E.; Bailey, V. L.; Simonson, C. J.; Saffarini, D. A.; Romine, M. F.; Zachara, J. M.; Fredrickson, J. K. *c*-Type cytochrome-dependent formation of U(IV) nanoparticles by *Shewanella oneidensis*. *PLoS Biol.* **2006**, *4*, e268.

(16) Campbell, K. M.; Veeramani, H.; Ulrich, K-. U.; Blue, L. Y.; Giammar, D. E.; Bernier-Latmani, R.; Stubbs, J. E.; Suvorova, E.; Yabusaki, S.; Lezama-Pacheco, J. S.; Mehta, A.; Long, P. E.; Bargar, J. R. Oxidative dissolution of biogenic uraninite in groundwater at Old Rifle, CO. *Environ. Sci. Technol.* **2011**, *45*, 8748−8754.

(17) Singh, A.; Ulrich, K. U.; Giammar, D. E. Impact of phosphate on U(VI) immobilization in the presence of goethite. *Geochim. Cosmochim. Acta* **2010**, *74*, 6324−6343.

(18) Ames, B. N. Assay of Inorganic Phosphate, Total Phosphate and Phosphatases. In: *Methods in Enzymology, Vol. VIII: Complex Carbohydrates*; Neufeld, E., Ginsburg, V., Eds.; Academic Press: New York, 1966 pp 115−118.

(19) Webb, S. M. SIXPACK: A graphical user interface for XAS analysis using IFEFFIT. *Phys. Scr.* **2005**, *T115*, 1011−1014.

(20) Ravel, B.; Newville, M. Athena, Artemis, Hephaestus: Data analysis for X-Ray absorption spectroscopy using Ifeffit. *J. Synchrotron Radiat.* **2005**, *12*, 537−541.

(21) Rehr, J. J.; Albers, R. C.; Zabinsky, S. I. High-order multiple-scattering calculations of X-ray-absorption fine-structure. *Phys. Rev. Lett.* **1992**, *69*, 3397−3400.

(22) Tylisczcak, T. Soft X-ray scanning transmission microscope working in an extended energy range at the Advanced Light Source. *Synchrotron Radiation Instrumentation 2003, AIP Conference Proceedings*, 2004; pp 1356−1359.

(23) Nilsson, H. J.; Tyliszczak, T.; Wilson, R. E.; Werme, L.; Shuh, D. K. Soft X-ray scanning transmission X-ray microscopy (STXM) of actinide particles. *Anal. Bioanal. Chem.* **2005**, *383*, 41−47.

(24) Rieger, D.; et al. Electronic-structure of the Caf2/Si(111) interface. *Phys Rev B.* **1986**, *34*, 7295−7306.

(25) Hitchcock, A. Chemical mapping with soft X-ray spectromicroscopy. *Am. Lab.* **2001**, *33*, 30−+.

(26) Jacobsen, C.; Wirick, S.; Flynn, G.; Zimba, C. Soft X-ray spectroscopy from image sequences with sub-100 nm spatial resolution. *J. Microsc.-Oxford* **2000**, *197*, 173−184.

(27) Jiang, W.; Saxena, A.; Song, B.; Ward, B. B.; Beveridge, T. J.; Myneni, S. C. B. Elucidation of functional groups on Gram-positive and Gram-negative bacterial surfaces using infrared spectroscopy. *Langmuir* **2004**, *20*, 11433−11442.

(28) Brooks, S. C.; Fredrickson, J. K; Carroll, S. L.; Kennedy, D. W.; Zachara, J. M.; Plymale, A. E.; Kelly, S. D.; Kemner, K. M.; Fendorf, S.

Inhibition of bacterial U(VI) reduction by calcium. *Environ. Sci. Technol.* **2003**, *37*, 1850−1858.
(29) Urich, K.; Veeremani, H.; Bernier-Latmani, R.; Giammar, D. E. Speciation dependent kinetics of uranium(VI) bioreduction. *Geomicrobiol. J.* **2011**, *28*, 396−409.
(30) Sheng, L.; Szymanowski, J.; Fein, J. B. The effects of uranium speciation on the rate of U(VI) reduction by *Shewanella oneidensis* MR-1. *Geochim. Cosmochim. Acta* **2011**, *75*, 3558−3567.
(31) Bargar, J. R.; Williams, K. H.; Campbell, K. M.; Long, P. E.; Stubbs, J. E.; Suvorova, E. I.; Lezama-Pacheco, J.; Alessi, D. S.; Stylo, M.; Webb, S. M.; Davis, J. A.; Giammar, D. E.; Blue, L. Y.; Bernier-Latmani, R. Uranium redox transition pathways in acetate-amended sediments. *Proc. Natl. Acad. Sci. U.S.A.* **2013**, *110* (12), 4506−4511.
(32) Finch, R. J.; Ewing, R. C. The corrosion of uraninite under oxidizing conditions. *J. Nucl. Mater.* **1992**, *190*, 133−156.
(33) Paige, C. R.; Snodgrass, W. J.; Nicholson, R. V.; Scharer, J. M.; He, Q. H. The effect of phosphate on the transformation of ferrihydrite into crystalline products in alkaline media. *Water, Air Soil Pollut.* **1997**, *97*, 397−412.
(34) Bocher, F.; Géhin, A.; Ruby, C.; Ghanbaja, J.; Abdelmoula, M.; Génin, J-M. R. Coprecipitation of Fe(II−III) hydroxycarbonate green rust stabilised by phosphate adsorption. *Solid State Sci.* **2004**, *6*, 117−124.
(35) Korenevsky, A.; Beveridge, T. J. The surface physicochemistry and adhesiveness of *Shewanella* are affected by their surface polysaccharide. *Microbiology* **2007**, *153*, 1872−1883.
(36) Vinogradov, E.; Korenevsky, A.; Beveridge, T. J. The structure of the rough-type lipopolysaccharide from *Shewanella oneidensis* MR-1, containing 8-amino-8-deoxy-Kdo and an open-chain form of 2-acetamido-2-deoxy-D-galactose. *Carbohydr. Res.* **2003**, *338*, 1991−1997.
(37) Subramaniam, S. B.; Yan, S.; Tyagi, R. D.; Surampalli, R. Y. Extracellular polymeric substances (EPS) producing bacterial strains of municipal wastewater sludge: Isolation, molecular identification, EPS characterization and performance for sludge settling and dewatering. *Wat. Res.* **2010**, *44*, 2253−2266.
(38) Subramaniam, S. B.; Yan, S.; Tyagi, R. D.; Surampalli, R. Y. Characterization of extracellular polymeric substances (EPS) extracted from both sludge and pure bacterial strains isolated from wastewater sludge for sludge dewatering. *Wat. Res.* **2007**, *12*, 1−7.
(39) Ha, J.; Gélabert, A.; Spormann, A. M.; Brown, A. M. Role of extracellular polymeric substances in metal ion complexation on Shewanella oneidensis: Batch uptake, thermodynamic modeling, ATR-FTIR, and EXAFS. *Geochim. Cosmochim. Acta* **2010**, *74*, 1−15.